Classical Chaos with Bose-Einstein Condensates in Tilted Optical Lattices

Quentin Thommen, Jean Claude Garreau, and Véronique Zehnlé

*Laboratoire de Physique des Lasers, Atomes et Molécules, Centre d'Etudes et de Recherches Laser et Applications, Université des Sciences et Technologies de Lille, F-59655 Villeneuve d'Ascq CEDEX, France**

(Received 24 June 2003; published 21 November 2003)

A widely accepted definition of "quantum chaos" is "the behavior of a quantum system whose classical limit is chaotic." The dynamics of quantum-chaotic systems is nevertheless very different from that of their classical counterparts. A fundamental reason for that is the linearity of Schrödinger equation. In this paper, we study the quantum dynamics of an ultracold quantum degenerate gas in a tilted optical lattice and show that it displays features very close to classical chaos. We show that its phase space is organized according to the Kolmogorov-Arnold-Moser theorem.

DOI: 10.1103/PhysRevLett.91.210405 PACS numbers: 03.75.Lm, 05.45.–a, 03.75.Kk

The quantum dynamics of systems presenting chaotic behavior in the classical limit has been a widely studied subject in recent years, boosted, in particular, by experiments using laser-cooled atoms [1–7]. An atomic-scale analog of the kicked rotor is realized by placing laser-cooled atoms in a pulsed standing laser wave, a system that displays a well-known signature of quantum chaos, the dynamical localization [8], present in time-periodic systems, which consists in the suppression of the classical chaotic diffusion by quantum interferences. Another well-known signature of quantum chaos, present in time-independent systems, is the fact that the distribution of energy levels takes the shape of a Wigner distribution, a behavior experimentally evidenced, for example, in the energy spectrum of Rydberg atoms in intense magnetic fields. This signature clearly cannot have a classical counterpart.

Quite generally, signatures of quantum chaos have no direct relation to the corresponding classical dynamics. There are fundamental reasons for this. One is that the notion of phase-space orbit, fundamental in classical dynamics, cannot be easily translated in the quantum world, due to the uncertainty principle. The initial conditions of a quantum system do not correspond to a single point in the usual phase space (q_i, p_i), as $\Delta q_i \Delta p_i \geq \hbar/2$. One can, however, project the state of the system in a basis, and define a generalized phase space formed by the set of amplitudes; if the basis is adequately chosen, the initial condition is represented by a point in such generalized phase space. Even then, sensitivity to initial conditions is not present, for the more fundamental reason that the Schrödinger equation is linear. Nonlinearity arises in classical physics because the dynamical variables (q_i, p_i) are also parameters of the force. In the case of the Schrödinger equation, the dynamical variable is the wave function, whereas the potential depends on (q_i, p_i), and eventually on t, but not on the wave function.

A Bose-Einstein condensate (BEC) is a quantum object described by a nonlinear quantum evolution equation, the Gross-Pitaevskii equation (GPE). GPE has proven to be able to describe the BEC dynamics with a reasonable precision on a wide range of situations [9]. GPE describes the condensate as whole (neglecting the noncondensed fraction), and includes a nonlinear term representing particle-particle interactions. It is valid for temperatures low enough compared to the critical temperature. If we consider a cigar-shaped BEC whose transverse length L is much smaller than the longitudinal length, the Gross-Pitaevskii equation can be reduced to one dimension, and reads

$$i\hbar \frac{\partial \psi}{\partial t} = (H_0 + U_0|\psi|^2)\psi, \tag{1}$$

where H_0 is the one-particle Hamiltonian, and U_0 a coupling constant describing the interaction among particles. U_0 is related to the two-particle s-wave scattering length a_s by $U_0 = 4\pi\hbar^2 a_s N/(L^2 M)$, where N is the total number of atoms, M is the mass of an atom, and the condensate wave function is normalized to unity. Contrary to the one-particle Schrödinger equation, this equation is nonlinear in the dynamical variable ψ. Note that, as $U_0 \propto N$, the GPE nonlinearity has a collective character: Modeling in an analogous way many-body interactions in an assembly of N thermal atoms would produce a much smaller nonlinear term.

The dynamics of one-dimensional, tilted, periodic potentials has often been considered in recent literature, both for free atoms [10–15], and for BECs [16–18]. A tilted optical potential,

$$V = V_0 \cos\left(\frac{2\pi x}{d}\right) + Fx, \tag{2}$$

is generated by superposing two counterpropagating laser waves, one of frequency $\omega_L = k_L c = 2\pi c/\lambda_L$ and the other of frequency $\omega_L(1 + \gamma t)$. This produces a standing wave of step $d = \lambda_L/2$ whose nodes are accelerated with an acceleration $c\gamma/2$. In the (noninertial) reference frame in which the nodes of the standing wave are at rest, an inertial force $F = -Mc\gamma/2$ appears, producing a "tilted" potential. In such a potential, quantum dynamics

consists in spatial oscillations over many steps of the potential, known as Bloch oscillations, as recently experimentally observed with both individual atoms [10] and (weakly interacting, low U_0) Bose-Einstein condensates [17].

We shall consider, in what follows, the particular form of the GPE given by

$$i\frac{\partial\psi(x,t)}{\partial t} = \left[-\frac{1}{2m}\frac{\partial^2}{\partial x^2} + V_0\cos(2\pi x) + Fx + g|\psi|^2\right]\psi, \tag{3}$$

where we introduced normalized units in which space is measured in units of the potential step d, energy in units of the recoil energy $E_R = \hbar^2 k_L^2/2M$, time in units of $\hbar/E_R$, force in units of $2E_R/\lambda_L$, $m = \pi^2/2$, and $g = 8a_s N/(L^2 k_L) = (2/\lambda_L)(U_0/E_R)$ is the (1D) nonlinear parameter ($\hbar = 1$ in such units). The eigenstates of the linear part of the Hamiltonian

$$H_0 = -\frac{1}{2m}\frac{\partial^2}{\partial x^2} + V_0\cos(2\pi x) + Fx \tag{4}$$

are the so-called Wannier-Stark (WS) states [19]. We assume that the depth of the potential V_0 is large enough to support well localized WS states, and that the dynamics can be described by the lowest-energy WS state in each well [15]. We note by φ_n the lowest state mainly localized in the nth well. The invariance of WS states under translations by an integer number of potential steps, $\varphi_n(x) = \varphi_0(x - n)$, is related to shifts of the eigenenergies given by $E_n = E_0 + nF$ (E_0 is an energy constant that can be eliminated), forming the so-called Wannier-Stark ladder of equally spaced levels [20], that define the Bloch (or Bohr) frequency of the system $\omega_B = Fd/\hbar$. Figure 1 displays an example of evolution of a BEC in a tilted potential, obtained by numerical integration via the split operator method [21], and the observed behavior suggests the existence of chaos in a classical sense.

In order to get a simpler description and a better understanding of the BEC dynamics, we now introduce a model obtained by projecting the wave function ψ over the WS states:

$$\psi(x,t) = \sum_n c_n(t)\varphi_n(x), \tag{5}$$

where the $c_n(t) \equiv \sqrt{I_n}e^{i\theta_n}$ are complex amplitudes. This development is justified provided that $g \lesssim 1$ [22], which corresponds, taking typical values for the parameters, to $N \simeq 7 \times 10^4$. Reporting Eq. (5) in Eq. (3) gives the evolution equation:

$$i\dot{c}_n = nFc_n + g\sum_{klm}\chi^n_{klm}c^*_k c_l c_m. \tag{6}$$

where the χ^n_{klm} are defined (choosing phases such that φ_n is a real function) by

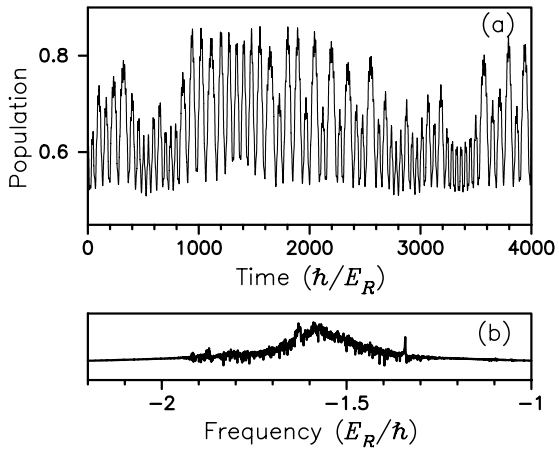

FIG. 1. Example of a chaotic evolution of a population. The BEC is initially prepared on three neighbor WS states around $n = 0$, with $I_{-1} = 0.1$, $I_0 = 0.6$, $I_1 = 0.3$, with phases $\varphi_{-1} = 0$, $\varphi_0 = 0$, $\varphi_1 = \pi$. Plot (a) displays the evolution of the population $I_0 = |\langle\varphi_0|\psi\rangle|^2$ of the central (most populated) well. Plot (b) displays the spectrum of this evolution. The result, obtained by numerical integration of the GPE, shows a chaotic behavior. Parameters are $V_0 = 5$, $F = 0.25$, and $g = 0.2$.

$$\chi^n_{klm} = \int_{-\infty}^{\infty}\varphi_k(x)\varphi_l(x)\varphi_m(x)\varphi_n(x)\,dx. \tag{7}$$

Because of invariance under discrete spatial translations of the WS states, one easily shows that $\chi^n_{k-n,l-n,m-n} = \chi^0_{klm} \equiv \chi_{klm}$ and, thus,

$$i\dot{c}_n = nFc_n + g\sum_{klm}\chi_{klm}c^*_{n+k}c_{n+l}c_{n+m}. \tag{8}$$

As WS are essentially localized in a well, we can keep only couplings between nearest neighbors, that is, involving χ_{000}, $\chi_{00\pm1}$ [23]. The equation of motion then simplifies to

$$\begin{aligned} i\dot{c}_n = {} & nFc_n + g\chi_{000}c_n|c_n|^2 \\ & + g(\chi_{00-1}c^*_{n-1} + \chi_{001}c^*_{n+1})c_n^2 \\ & + g(2\chi_{00-1}c_{n-1} + 2\chi_{001}c_{n+1})|c_n|^2 \\ & + g(\chi_{001}|c_{n-1}|^2c_{n-1} + \chi_{00-1}|c_{n+1}|^2c_{n+1}), \end{aligned} \tag{9}$$

where we used the invariance of the χ_{klm} coefficients under any permutation of indexes. Figure 2 displays the evolution obtained from the model, for the same parameters and the same initial conditions as in Fig. 1. The temporal evolution is not identical to that shown in Fig. 1 because of the sensitivity of chaotic evolution to small perturbations, but the dynamical behavior has the same characteristics. This is better evidenced by comparing the spectra of both evolutions, shown in part (b) of the figures. The model is thus able to reproduce the dynamics of the GPE.

It is useful to write evolution equations for the population $I_n = |c_n|^2$ and the phase θ_n:

$$\begin{aligned} \dot{I}_n = {} & 2\varepsilon\sigma_g\sqrt{I_n}[\sqrt{I_{n+1}}(I_{n+1} + \beta I_n)\sin(\theta_{n+1} - \theta_n) \\ & + \sqrt{I_{n-1}}(I_n + \beta I_{n-1})\sin(\theta_{n-1} - \theta_n)], \end{aligned} \tag{10}$$

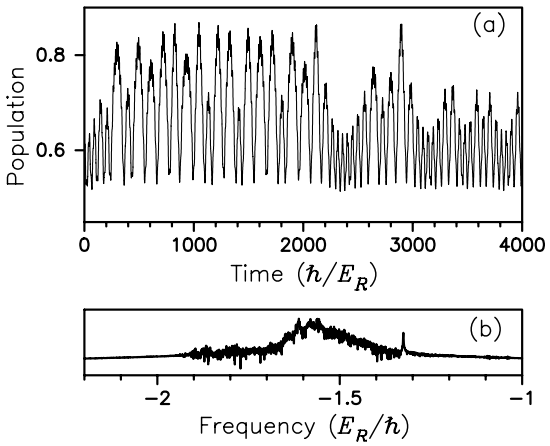

FIG. 2. Same as Fig. 1, but the calculation was made using the discrete model of Eq. (9). Plot (a) displays the same kind of chaotic dynamics as in Fig. 1, and plot (b) shows that the spectrum of the evolution is virtually the same.

$$\dot{\theta}_n = -nF - \sigma_g I_n - \frac{\varepsilon\sigma_g}{\sqrt{I_n}}[\sqrt{I_{n+1}}(I_{n+1} + 3\beta I_n)\cos(\theta_{n+1} - \theta_n) - \sqrt{I_{n-1}}(3I_n + \beta I_{n-1})\cos(\theta_{n-1} - \theta_n)], \tag{11}$$

with $\sigma_g = g/|g|$, $\beta = \chi_{001}/\chi_{00-1} \approx -1$, and we have rescaled the time variable as $t \to t/(|g|\chi_{000})$ and the force as $F \to F/(|g|\chi_{000})$. Parameter $\varepsilon = \chi_{00-1}/\chi_{000}$ is small since $\chi_{00-1}/\chi_{000} \ll 1$ [23]. If we neglect interwell particle interactions, i.e., for $\varepsilon = 0$, all $I_n = I_n(0)$ are constants of motion, and $\theta_n = \theta_n(0) + \omega_n t$ increases linearly with time with frequency $\omega_n = -nF - \sigma_g I_n$. The variables (I_n, θ_n) have then an "action-angle" structure [24] and the system is integrable. The trajectories lay on tori defined by the values of the constants of motion [25]. In usual units, the frequencies ω_n are

$$\omega_n = n\omega_B + \frac{U_0\chi_{000}}{\hbar} I_n, \tag{12}$$

where the second term on the right-hand side represents a "frequency pulling" effect due to the nonlinearity. Moreover, one can verify that Eqs. (10) and (11) can be obtained by the usual prescription, $\dot{I}_n = (\partial H)/(\partial\theta_n)$ and $\dot{\theta}_n = -(\partial H)/(\partial I_n)$ from the Hamiltonian given by

$$H = \sum_n [nFI_n + \frac{\sigma_g}{2} I_n^2 + 2\sigma_g\varepsilon\sqrt{I_n I_{n+1}}(\beta I_n + I_{n+1}) \times \cos(\theta_{n+1} - \theta_n)] = H_0(I) + \varepsilon\sum_n [V_n(I)\cos(\theta_{n+1} - \theta_n)]. \tag{13}$$

The Hamiltonian is the sum of an integrable part and a nonintegrable "perturbation." This form strongly evokes the Kolmogorov-Arnold-Moser (KAM) theorem [25]. If $0 < \varepsilon \ll 1$, the system is said to be quasi-integrable and the KAM theorem states that the tori are only slightly deformed if initially the system is far from its resonances. A resonance is defined by $\sum_n \ell_n\omega_n = 0$, with ℓ_n integer. Note that the KAM-like structure of our system depends only on the smallness of the parameter ε, which can be modified by changing the properties of the potential.

In order to illustrate the above conclusions, consider the simple case in which the BEC initially projects only on three adjacent WS states, labeled -1, 0, 1. During the evolution, the spread of the wave function to other WS states is very small [26]. We performed a numerical integration of the equations of motion and plotted a Poincaré section [of the generalized phase-space (I, θ)], corresponding to the plane $(I_0, \theta_1 - \theta_0)$, displayed in Fig. 3, which presents characteristic features of a classically chaotic system, despite the fact that a BEC is a quantum object.

A principal resonance is observed when the ratio of two frequencies is a rational number, e.g., $\omega_n/\omega_m = a/b$ (a and b integers). The simplest case, $a = b = 1$, called "1:1" resonance, corresponds to the resonance condition [cf. Equation (12)]

$$\hbar\omega_B = U_0\chi_{000}(I_0 - I_1). \tag{14}$$

for the two neighbor sites $n = 0$, $m = 1$. It has a simple interpretation: The energy levels corresponding to the two wells become quasidegenerate due to the nonlinear shift, thus favoring population exchanges. Higher order resonances affect smaller regions of the phase space. Thus, in order to observe chaotic behavior, the initial wave function shall not be too smoothly distributed on the lattice: If all I_n are almost identical, only higher order resonances will show up. The arrow in Fig. 3 indicates the 1:1 resonance, which is surrounded by other signatures of frequency locking, characterized by the presence of

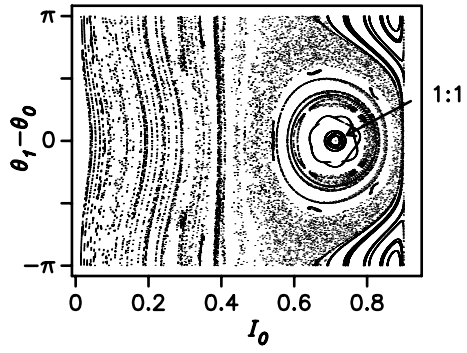

FIG. 3. Poincaré section of the generalized (quantum) phase space, corresponding to the plane $(I_0, \theta_1 - \theta_0)$. The plane is defined by $I_{-1} = 0.1$, $\theta_{-1} = \theta_0$, all other angles and actions are zero, except $I_1 = 0.9 - I_0$, imposed by the normalization condition. One observes different types of dynamics, ranging from regular to chaotic. The arrow indicates the 1:1 resonance, and one can see around it various frequency-locking signatures evidenced by the presence stability islands. We verified that the calculations made either with the discrete model or by direct numerical integration of the GPE produce the same topology. Parameters are the same as in Fig. 1, except that $g = 0.25$.

stability islands. The groups of three and five stability islands correspond, respectively, to the resonances 3:1 and 5:1. The quantum phase space has thus a KAM-like structure. Far from resonances, regular motion is displayed (left part of the Poincaré section). In this case, the nonlinearity introduces population-dependent frequencies due to the frequency pulling effect. The emergence of these frequencies eventually blur Bloch oscillations (which would correspond to vertical straight lines).

In conclusion, we have presented in this paper a quantum system that displays a behavior very similar to classical chaos, thanks to the presence of a nonlinearity due to many-body interactions (studies of chaotic dynamics in other quantum systems can be found, e.g., in Refs. [27–29]). As we emphasized above, this is not quantum chaos, at least in the most widely accepted definition of the term. It is closer to classical Hamiltonian chaos, except for the fact that it is observed in a generalized phase space. The structure of the phase space can be interpreted in the general frame of the KAM theorem. This leaves open many stimulating questions: Are the conditions leading to the Gross-Pitaevskii approach essential for observing "classical" chaos with a BEC, or can the same phenomenon manifest itself in less restrictive conditions? What are the necessary and sufficient conditions for observing classical chaos with BECs? Can one find experimentally realizable situations in which a quantum effect (e.g., quantum interference) coexists with chaos, and how will chaos affect it? How is classical chaos with BECs affected by decoherence? These few questions suggest that the present work opens an interesting way for investigations of the quantum-classical limit in mesoscopic systems.

The authors are indebted to D. Delande for fruitful discussions. This work is partially supported by a contract "ACI Photonique." Laboratoire de Physique des Lasers, Atomes et Molécules (PhLAM) is Unité Mixte de Recherche UMR 8523 du CNRS et de l'Université des Sciences et Technologies de Lille.

*URL: http://www.phlam.univ-lille1.fr/atfr/cq

[1] F. L. Moore, J. C. Robinson, C. F. Bharucha, P. E. Williams, and M. G. Raizen, Phys. Rev. Lett. **73**, 2974 (1994).
[2] H. Ammann, R. Gray, I. Shvarchuck, and N. Christensen, Phys. Rev. Lett. **80**, 4111 (1998).
[3] M. K. Oberthaler, R. M. Godun, M. B. Darcy, G. S. Summy, and K. Burnett, Phys. Rev. Lett. **83**, 4447 (1999).
[4] D. A. Steck, W H. Oskay, and M. G. Raizen, Science **293**, 274 (2001).
[5] W. K. Hensinger *et al.*, Nature (London) **412**, 52 (2001).
[6] J. Ringot, P. Szriftgiser, J. C. Garreau, and D. Delande, Phys. Rev. Lett. **85**, 2741 (2000).
[7] P. Szriftgiser, J. Ringot, D. Delande, and J. C. Garreau, Phys. Rev. Lett. **89**, 224101 (2002).
[8] G. Casati, B. V. Chirikov, J. Ford, and F. M. Izrailev, Lect. Notes Phys. **93**, 334 (1979).
[9] F. Dalfovo, S. Giorgini, L. Pitaevskii, and S. Stringari, Rev. Mod. Phys. **71**, 463 (1999).
[10] M. Ben Dahan, E. Peik, J. Reichel, Y. Castin, and C. Salomon, Phys. Rev. Lett. **76**, 4508 (1996).
[11] M. Glück, A. R. Kolovsky, and H. J. Korsch, Phys. Rev. Lett. **83**, 891 (1999).
[12] M. Glück, F. Keck, and H. J. Korsch, Phys. Rev. A **66**, 043418 (2002).
[13] M. Glück, A. R. Kolovsky, and H. J. Korsch, Phys. Rep. **366**, 103 (2002).
[14] H. L. Haroutyunyan and G. Nienhuis, Phys. Rev. A **64**, 033424 (2001).
[15] Q. Thommen, J. C. Garreau, and V. Zehnlé, Phys. Rev. A **65**, 053406 (2002).
[16] B. P. Anderson and M. Kasevich, Science **282**, 1686 (1998).
[17] O. Morsch, J. H. Mueller, M. Cristiani, D. Ciampini, and E. Arimondo, Phys. Rev. Lett. **87**, 140402 (2001).
[18] A. Trombettoni and A. Smerzi, Phys. Rev. Lett. **86**, 2353 (2001).
[19] This is rigorously true if the whole system is enclosed in a bounding box of dimensions much larger than d; otherwise, WS states must be considered as metastable states (resonances).
[20] These symmetries are approximate for WS states in a bounding box, but they apply with a good precision to states far from the bounding box.
[21] M. D. Feit, J. A. Fleck, and A. Steiger, J. Comput. Phys. **47**, 412 (1982).
[22] Numerical integration of Eq. (3) shows that the expansion [see Eq. (5)] of $\psi(x)$ over first-band states $\varphi_n(x)$ remains valid for values of g as high as $g = 1$. More precisely, if at $t = 0$ the wave packet is prepared in a superposition of such states, so that $\sum_n |c_n(t = 0)|^2 = 1$, after a typical evolution time t we find $\sum_n |c_n(t)|^2 = 1 - \varepsilon$, with $\varepsilon \approx 0.02$. This shows the BEC dynamics is essentially confined to the first band, and that considering only such states is a very good approximation.
[23] For the typical parameters we are dealing with, $V_0 = 5$ and $F = 0.25$, one obtains $\chi_{000} \approx 1.99$, $\chi_{001} \approx -0.16$, and $\chi_{00-1} \approx 0.15$. Other couplings are much smaller.
[24] O. Zobay and B. M. Garraway, Phys. Rev. A **61**, 033603 (2000).
[25] M. C. Gutzwiller, *Chaos in Classical and Quantum Mechanics* (Springer-Verlag, Berlin, 1986).
[26] Population transfer between wells occurs if the nonlinear frequency shift brings the energy levels of neighbor wells into degeneracy [cf. Eq. (14)]. This condition cannot be satisfied for wells with a low population.
[27] Y. Ashkenazy, L. P. Horwitz, J. Levitan, M. Lewkowicz, and Y. Rothschild, Phys. Rev. Lett. **75**, 1070 (1995).
[28] R. Blümel and B. Esser, Phys. Rev. Lett. **72**, 3658 (1994).
[29] I. Barvik, B. Esser, and H. Schanz, Phys. Rev. B **52**, 9377 (1995).